Energy Engineering

Tech Science Press

Doi:10.32604/ee.2025.074707

ARTICLE

Photovoltaic Output Prediction and Trading Strategy Based on Fractal Theory

Yifeng Wang[1,*], Wei Cui[1], Zhihui Wang[2], Yanning Xue[2] and Bing Wang[2]

[1]State Grid Hebei Electric Power Co., Ltd., Shijiazhuang, 050023, China
[2]State Grid Hebei Electric Power Co., Ltd., Hengshui Power Supply Branch, Hengshui, 050022, China

*Corresponding Author: Yifeng Wang: Email: wangyifeng0817@163.com

Received: 16 October 2025; Accepted: 26 November 2025; Published: 30 August 2026

ABSTRACT: This paper proposes a photovoltaic (PV) output prediction and trading strategy based on fractal theory. Firstly, rescaled range analysis (R/S analysis) is employed to quantify the fractal characteristics of PV output sequences under different weather conditions. By calculating the Hurst exponent and fractal dimension, the self-similarity patterns and complexity differences are revealed. Secondly, a fractal interpolation prediction method based on the iterated function system is constructed to achieve high-precision fitting of typical daily output curves. Finally, by integrating the fractal prediction results, a trading decision-making model aimed at minimizing daily electricity procurement costs is established, and a dynamic pricing mechanism linked to the spot market price is designed to coordinate and optimize the PV consumption ratio and spot market procurement strategy. Case study analysis demonstrates that the proposed strategy can effectively improve the PV consumption rate and reduce the procurement costs for electricity retailers, providing reliable technical support for distributed PV to participate in electricity market trading.

KEYWORDS: Fractal theory; distributed photovoltaic; output prediction; trading strategy

1 Introduction

Driven by the “dual carbon” goals, the transformation of the energy structure is accelerating. With their clean and renewable advantages, PV power generation has become a core force in upgrading the global energy system [1–4]. In recent years, the penetration of distributed PVs on the distribution grid side has continued to increase. Their large-scale grid integration provides important support for the low-carbon development of the energy system, but also brings new technical challenges [5,6]. The traditional electricity market has been dominated by centralized power generation, with grid companies holding an absolute dominant position in unified purchasing and selling. However, with the continuous development of the energy industry and the reform of the electricity retail market, competitive services have been gradually liberalized, leading to the rapid emergence of user-side distributed PVs [7–10]. Many users have installed PV equipment, significantly increasing the sensitivity of their electricity purchasing demand to selling prices. This growing price elasticity has become increasingly evident and profoundly influences electricity purchasing and selling decisions.

In recent years, the application of fractal theory in energy system analysis has gradually gained attention, demonstrating unique advantages in fields such as wind power prediction and load characteristic analysis. The core of fractals lies in revealing structures that exhibit self-similarity across different scales, meaning the local and global aspects show high consistency in morphology, function, or statistical characteristics. In renewable energy power systems, the intermittency, volatility, and uncertainty of PV power output have always been key issues restricting its large-scale grid integration. Traditional deterministic or statistical models often struggle to fully describe its inherent complex behaviors, while fractal theory provides a new perspective and methodology, capable of uncovering the underlying regularity behind PV output fluctuations at a deeper level [11–14]. Fractal theory, as a powerful tool for studying complex, nonlinear, and scale-invariant systems, has demonstrated its unique value in multiple scientific and engineering fields. Its core lies in revealing the self-similarity exhibited by the system at different scales. In financial time series analysis, fractal methods are widely used to depict the long-range dependence and multifractal characteristics of price fluctuations. Reference [15] utilized the weighted range analysis to reveal the inherent memory of market fluctuations. In recent years, the application of this theory has extended to the field of solar physics, by calculating the Hurst index and analyzing the persistent influence of solar activity on ionospheric changes, proving the effectiveness of fractal measures in characterizing the dynamic evolution of spatial physical phenomena. These interdisciplinary successful applications indicate that fractal theory provides a universal framework for understanding systems with inherent complexity, non-stationarity, and multi-scale characteristics. However, research on fractal theory-based PV output prediction remains in the exploratory stage.

As a key player in the electricity retail market, electricity retailers generate profits through the price difference between electricity sales and purchases. Therefore, minimizing procurement costs has become a core task for retailers to enhance market competitiveness and profitability. In [16], the electricity pricing mechanisms were investigated, which involved market operators, residential PV systems, energy storage devices, producer-consumers, and conventional consumers, and a two-stage decision framework was proposed to maximize profits. In [17], an optimized power procurement and sales model was developed by using a Stackelberg game to coordinate electricity strategies between operators and PV users, thereby improving renewable energy integration. In [18], an optimization method for the competitiveness decision of electricity retailers was proposed, two types of electricity service packages, namely the general service package and the customized service package, were designed, and the electricity trading plan in the electricity market was formulated. When not engaged in distributed PV agency services, electricity retailers primarily rely on medium-long-term contracts to hedge against spot market price risks. These contracts can lock in procurement prices to some extent, reducing cost uncertainties caused by extreme spot market fluctuations. However, with the widespread adoption of distributed PV, retailers acting as PV agents must now holistically consider both PV generation patterns and spot price volatility to optimize their electricity procurement strategies.

The power output of distributed PV systems exhibits distinct diurnal fluctuations and demonstrates certain correlations with spot market price variations [19–22]. By strategically coordinating the proportion of distributed PV generation and spot market procurement, electricity retailers can achieve daily cost minimization in power purchases. In this process, the price market feedback mechanism significantly influences the penetration rate of distributed PV. In [23], a reactive power market mechanism was designed, and an iterative algorithm was developed to calculate the Nash equilibrium of the proposed market and quantify the market concentration, and proved the applicability of the proposed algorithm in different distribution systems. In [24], a spot market trading mechanism was designed to resolve the conflict between high-penetration renewable energy participation in market competition and guaranteed consumption. In an ideal electricity retail market environment, distributed PV systems, end-users, electricity retailers, and regulatory authorities form a closed-loop feedback system [25–28]. However, under the coordinated electricity retail model, electricity retailers face multiple challenges in optimizing procurement strategies and aligning interests with distributed photovoltaic systems [29,30]. Power retailers must optimize procurement by comparing spot forecasts with PV contract prices to set bidding curves and generation schedules.

Yet conventional fixed-price contracts fail to handle spot market volatility, causing sub-optimal decisions that reduce PV utilization or raise costs.

The sequence of photovoltaic output is affected by multiple natural factors and exhibits non-stationary, non-linear, and multi-time-scale fluctuation characteristics. A large number of studies have shown that such sequences have statistical self-similarity at different time scales, that is, there is similarity between local fluctuation patterns and overall behavior, which conforms to the basic assumptions of the fractal theory. Therefore, using the fractal theory to model the photovoltaic output can better capture its inherent complex dynamic behavior.

Based on the above analysis, this paper proposes a PV output prediction and trading strategy based on fractal theory. Firstly, R/S analysis is employed to quantify the fractal characteristics of PV output sequences under different weather conditions, revealing their self-similarity patterns and complexity variations. Secondly, a fractal interpolation-based forecasting method is proposed to achieve high-precision fitting of typical daily output curves. Furthermore, a dynamic pricing and decision optimization model is constructed to collaboratively optimize electricity procurement costs and PV consumption. Finally, case studies are conducted to verify the reliability and applicability of the proposed methodology.

2 Materials and Methods

2.1 Fractal Characteristics Analysis of PVs

A fractal is a set with infinitely fine structure that exhibits self-similarity across different scales. Its core characteristics include: (1) Self-similarity. The local and global parts are highly consistent in morphology and statistical characteristics. For instance, fluctuation patterns in PV output curves are similar across intra-day and multi-day scales. (2) Non-integer dimension. The fractal dimension (D) lies between integer dimensions and can quantify the complexity of output fluctuations—a higher D value indicates more intense volatility. (3) Iterative generation. Complex output curves can be generated through simple mathematical rules.

Rescaled range analysis (R/S analysis) was first proposed by hydrologist Hurst (1951) when he was studying the capacity of the Nile River reservoir, to quantify the long-range correlation and long-term memory effect of time series. This method was later systematically introduced into fractal geometry and economic research and developed into one of the standard tools for analyzing the fractal characteristics of nonlinear and non-stationary time series. The core lies in calculating the Hurst index (H) to distinguish random sequences from fractal sequences with persistence/anti-persistence.

Given a sequence $Z = \{R_t: t = 1, 2, \ldots, M\}$ of length M, the entire sequence is divided into B sub-intervals of length m. Each sub-interval is denoted as I_s, $s = 1, 2, \ldots, B$, and each element in I_s is denoted as $R_{k,s}$, $k = 1, 2, \ldots, m$; $s = 1, 2, \ldots, B$.

For each sub-interval I, the mean value is calculated as:

$$E_s = \frac{\sum_{k=1}^{m} R_{k,s}}{m} \tag{1}$$

Next, the cumulative deviation of each point relative to this mean value is calculated as:

$$X_{k,s} = \sum_{k=1}^{m} \left(R_{k,s} - E_s \right) \tag{2}$$

Then, the range of each sub-interval is calculated as:

$$R_{I_s} = \max_k (X_{k,s}) - \min_k (X_{k,s}), \ k = 1, 2, \cdots, m \tag{3}$$

Next, the standard deviation of each sub-interval is calculated as:

$$S_{I_s} = \sqrt{\frac{1}{m}\sum_{k=1}^{m} (R_{I_s} - E_s)^2} \tag{4}$$

For a given length m, the average rescaled range across all sub-intervals is calculated as:

$$(R/S)_m = \frac{1}{B}\sum_{s=1}^{B} \frac{R_{I_s}}{S_{I_s}} \tag{5}$$

By selecting different values of m, multiple average rescaled ranges can be obtained. Taking the logarithm of Eq. (5) yields:

$$\log\left[(R/S)_m\right] = \log(C) + H\log(m) \tag{6}$$

By performing linear regression with $\log(m)$ as the independent variable and $\log[(R/S)_m]$ as the dependent variable, the slope of the fitted line corresponds to the Hurst exponent (H). After obtaining H, the fractal dimension can be expressed as: $D = 2 - H$.

2.2 PV Output Forecasting Based on Fractal Interpolation

Fractal interpolation is a method for constructing fractal curves based on iterated function systems (IFS). By establishing an IFS corresponding to the interpolation points, the attractor of the system forms a function graph that passes through these points, thereby overcoming the smoothness constraints of traditional interpolation methods.

Given a set of data points $\{(x_i, y_i) \in R^2: i = 0, 1, 2, \ldots, N\}$, an IFS consisting of N affine transformations $\{(w_j): j = 0, 1, 2, \ldots, N\}$ is constructed. Each transformation w_j maps the entire interval $[x_0, x_N]$ onto the sub-interval $[x_{j-1}, x_j]$, while simultaneously applying vertical stretching and shifting. The affine transformation w_j takes the form:

$$w_j\begin{bmatrix} x \\ y \end{bmatrix} = \begin{bmatrix} a_j & 0 \\ c_j & d_j \end{bmatrix}\begin{bmatrix} x \\ y \end{bmatrix} + \begin{bmatrix} e_j \\ f_j \end{bmatrix} \tag{7}$$

For each transformation w_j, it is required to map the first point to the starting point of the current segment and the last point to the endpoint of the current segment. That is:

$$w_j\begin{bmatrix} x_0 \\ y_0 \end{bmatrix} = \begin{bmatrix} x_{j-1} \\ y_{j-1} \end{bmatrix} \text{ and } w_j\begin{bmatrix} x_N \\ y_N \end{bmatrix} = \begin{bmatrix} x_j \\ y_j \end{bmatrix}$$

Each transformation must satisfy:

$$\begin{cases} a_j x_0 + e_j = x_{j-1} \\ a_j x_N + e_j = x_j \\ c_j x_0 + d_j y_0 + f_j = y_{j-1} \\ c_j x_N + d_j y_N + f_j = y_j \end{cases} \tag{8}$$

Eq. (8) contains four equations with five unknown parameters. In the definition of the fractal interpolation algorithm, the matrix transformation is essentially a stretching operation. It maps a line segment originally parallel to the y-axis to another line segment also parallel to the y-axis. During this mapping process, the ratio of the length of the original segment to that of the new segment is d_j, known as the vertical scaling factor. d_j is a real number between 0 and 1 that determines the "roughness" or "irregularity" of the generated curve. When $d_j = 0$, the method degenerates to simple linear interpolation. The closer $|d_j|$ is to 1, the more fluctuations and details the generated curve exhibits over the sub-interval. By selecting d_j as the free variable, the solution to Eq. (8) can be obtained as:

$$\begin{cases} a_j = \left(x_j - x_{j-1}\right) / \left(x_N - x_0\right) \\ e_j = \left(x_N x_{j-1} - x_0 x_j\right) / \left(x_N - x_0\right) \\ c_j = \left[y_j - y_{j-1} - d_j\left(y_N - y_0\right)\right] / \left(x_N - x_0\right) \\ f_j = \left[x_N y_{j-1} - x_0 y_j - d_j\left(x_N y_0 - x_0 y_N\right)\right] / \left(x_N - x_0\right) \end{cases} \tag{9}$$

From Eq. (9), the j-th affine transformation in the IFS can be derived, thereby obtaining the attractor of the IFS. As the number of iterations increases, the fitted curve obtained through interpolation progressively better approximates the original sampled curve. After multiple iterations, a stable invariant interpolation curve is formed. Compared with traditional interpolation methods, fractal interpolation addresses their inability to capture local features between adjacent known data points. The generated interpolation curve not only passes through the sampled interpolation points but also retains most characteristics of the original sampled curve while exhibiting rich detailed information. Compared with traditional ARIMA models and deep learning methods such as LSTM, the fractal interpolation method does not rely on the assumption of stationarity of the sequence and does not require a large amount of training data. It can reconstruct output curves with rich details using a small number of interpolation points and is more suitable for describing the nonlinear and multi-scale fluctuation characteristics of photovoltaic output.

2.3 PV Market Trading Mechanism Integrating Fractal Prediction

2.3.1 Electricity Retailer Cost Model

After a electricity retail company integrates distributed PV resources, it must correlate the diurnal output characteristics of PV generation with fluctuations in spot market prices. By optimizing the balance between PV consumption and spot market procurement, the company aims to minimize daily electricity procurement costs. Consequently, the load profile managed by the retail company must satisfy the following conditions:

$$P_{\mathrm{s}}^{(t)} = \sum_{i=1}^{N_1} P_{\mathrm{L},i}^{(t)} - \sum_{j=1}^{N_2} P_{\mathrm{PV},j}^{(t)} \tag{10}$$

where $P_{\mathrm{s}}^{(t)}$ is the electricity procurement power of the retailer at time t, $P_{\mathrm{L},i}^{(t)}$ is the load demand power of user i at time t, $P_{\mathrm{PV},j}^{(t)}$ is the output power of PV j at time t.

This paper considers two primary types: fixed loads and flexible loads, where flexible loads include interruptible loads and shiftable loads. Thus, the expression becomes:

$$\begin{aligned}
&P_{\mathrm{L},i}^{(t)} = P_{\mathrm{Lnl},i}^{(t)} + P_{\mathrm{Lml},i}^{(t)} + P_{\mathrm{Lsl},i}^{(t)} \\
&0 \le P_{\mathrm{Lml},i}^{(t)} \le P_{\mathrm{Lml},i}^{0} \\
&-P_{\mathrm{Lsl},i}^{0} \le P_{\mathrm{Lsl},i}^{(t)} \\
&\sum_{t\in T} P_{\mathrm{Lsl},i}^{(t)} = 0
\end{aligned} \tag{11}$$

where $P_{\mathrm{Lnl},i}^{(t)}$ is the fixed load of user i at time t, $P_{\mathrm{Lml},i}^{(t)}$ is the interruptible load of user i at time t, $P_{\mathrm{Lsl},i}^{(t)}$ is the shiftable load of user i at time t, $P_{\mathrm{Lml},i}^{0}$ is the initial interruptible load capacity of user i, $P_{\mathrm{Lsl},i}^{0}$ is the initial shiftable load capacity of user i, T is the load shifting cycle.

The electricity retail company determines its procurement volume based on PV output and user demand. The electricity procurement cost can be expressed as:

$$C_{\mathrm{G}} = \sum_{t=1}^{T_D} \left(P_{\mathrm{s}}^{(t)} E_{\mathrm{s}}^{(t)} \Delta t + \sum_{j=1}^{N_2} P_{\mathrm{PV},j}^{(t)} E_{\mathrm{PV}}^{(t)} \Delta t \right) \tag{12}$$

where $E_{\mathrm{s}}^{(t)}$ is the market electricity price at time t, T_D is the procurement cycle duration, Δt is the time interval, $E_{\mathrm{PV}}^{(t)}$ is the PV electricity price.

2.3.2 Electricity Retail Trading Decision Model

The electricity retail company aggregates the managed distributed PV resources and energy storage systems into an equivalent single generation unit. By charging the storage during low-price periods and discharging during high-price periods, the company leverages electricity price differentials to minimize procurement costs. In the spot market, with the objective of minimizing electricity procurement costs, the electricity retail company establishes the following transaction decision objective function:

$$\min \ C = \sum_{t=1}^{T_D} \left[\left(P_{\mathrm{PV},j}^{(t)} + P_{\mathrm{sdis}}^{(t)} \right) E_{\mathrm{PV}}^{(t)} \Delta t + P_{\mathrm{s}}^{(t)} E_{\mathrm{s}}^{(t)} \Delta t \right] \tag{13}$$

where $P_{\mathrm{sdis}}^{(t)}$ is the energy storage discharge power at time t.

The main constraint conditions that the objective function needs to satisfy include:

(1) Power balance constraint:

$$P_{\mathrm{s}}^{(t)} + P_{\mathrm{sdis}}^{(t)} + \sum_{j=1}^{N_2} P_{\mathrm{PV},j}^{(t)} = \sum_{i=1}^{N_1} P_{\mathrm{L},i}^{(t)} + P_{\mathrm{sch}}^{(t)} \tag{14}$$

where $P_{\mathrm{sch}}^{(t)}$ is the energy storage charging power at time t.

(2) Energy storage operation constraints:

$$0 \le P_{\mathrm{sdis}}^{(t)} \le P_{\mathrm{sdis}}^{\max} \tag{15}$$

$$0 \le P_{\mathrm{sch}}^{(t)} \le P_{\mathrm{sch}}^{\max} \tag{16}$$

$$S_{\mathrm{SOC}}^{(t)} = S_{\mathrm{SOC}}^{(t-1)} + P_{\mathrm{sch}}^{(t)}\eta_{\mathrm{sch}} - P_{\mathrm{sdis}}^{(t)}\eta_{\mathrm{sdis}} \tag{17}$$

$$E_{\mathrm{s}}^{\min} \le E_{\mathrm{s}}^{(t)} \le E_{\mathrm{s}}^{\max} \tag{18}$$

$$S_{\mathrm{SOC}}^{(0)} = S_{\mathrm{SOC}}^{(T_{\mathrm{soc}})} \tag{19}$$

where $P_{\mathrm{sdis}}^{\max}$ is maximum allowable discharge power of the energy storage system (ESS), $P_{\mathrm{sch}}^{\max}$ is maximum allowable charge power of ESS, $S_{\mathrm{SOC}}^{(t)}$ is State of charge of ESS at time t, η_{sch} and η_{sdis} are charging and discharging efficiencies of ESS, respectively, $E_{\mathrm{s}}^{(t)}$ is Available energy capacity of ESS at time t, $E_{\mathrm{s}}^{\min}$ and $E_{\mathrm{s}}^{\max}$ are the minimum and maximum energy capacity limits of ESS, respectively, T_{soc} is storage cycle duration.

(3) PV power output constraints:

$$0 \le P_{\mathrm{PV},j}^{(t)} \le P_{\mathrm{PV},j}^{\max} \tag{20}$$

where $P_{\mathrm{PV},j}^{\max}$ is maximum output power of PV j.

2.3.3 Pricing and Trading Strategy

The effectiveness of the electricity trading decision model depends on the dynamic spread between the contract price and the spot price. By adopting a dynamic pricing mechanism linked to day-ahead predicted electricity prices, and establishing mathematical correlations that allow prices to reflect market supply and demand, the efficiency of resource allocation is enhanced. Assuming the electricity retail company's forecast for the day-ahead electricity price is represented as:

$$\mathbf{E}_{\mathrm{da}} = \left[E_{\mathrm{pr}}^{1}, E_{\mathrm{pr}}^{2}, \cdots, E_{\mathrm{pr}}^{T_D}\right] \tag{21}$$

where $E_{\mathrm{pr}}^{T_D}$ is the predicted electricity price for time period t.

Based on the electricity price forecasts by the retail company, the average electricity price for the entire day and the average price during the evening peak period can be calculated respectively as:

$$E_{\mathrm{ave}} = \frac{\sum_{i=1}^{T_D} E_{\mathrm{pr}}^{i}}{T_D} \tag{22}$$

$$E_{\mathrm{night}} = \frac{\sum_{i \in T_{\mathrm{n}}} E_{\mathrm{pr}}^{i}}{T_{\mathrm{n}}} \tag{23}$$

where E_{ave} is the average daily electricity price, E_{night} is he average electricity price during the evening peak period, T_{n} is the number of time intervals in the peak period.

To facilitate analysis, using the average daily electricity price as a reference, a proportionality coefficient c is defined as:

$$c = \frac{E_{\mathrm{night}}}{E_{\mathrm{ave}}} \tag{24}$$

The dynamic pricing mechanism defines the price variation range as $[E_{\mathrm{ave}}, E_{\mathrm{night}}]$, and uses the proportionality coefficient c to determine the final optimized decision price. When the agreement factor $1 \le \delta \le c$ is satisfied, it indicates that the optimized decision price is c times the day-ahead average electricity price.

Using predicted electricity prices as the settlement benchmark has inherent limitations: prediction deviations lead to asymmetric risks, violate market fairness principles, and may trigger strategic countermeasures. To balance the interests of both parties, this paper proposes a settlement mechanism based on actual clearing prices, using the daily actual average clearing price as a reference to establish an actual proportionality coefficient as:

$$c_{\text{rea}} = \frac{E_{\text{rea\_night}}}{E_{\text{rea\_ave}}} \tag{25}$$

where $E_{\text{rea\_night}}$ is the actual average electricity price during the evening peak period, $E_{\text{rea\_ave}}$ is the actual average electricity price.

This mechanism anchors the photovoltaic settlement price to the actual clearing price, ensuring that prices accurately reflect market value and eliminating prediction deviations. It not only safeguards the cost optimization benefits for electricity retailers, maintaining their market participation incentives, but also achieves incentive compatibility through the "quantity-guaranteed but price-unguaranteed" principle. The linkage of revenues with the real-time market encourages improvements in forecasting accuracy, while the separation of quantity and price prevents policy arbitrage, forming a virtuous cycle between technological advancement and market efficiency. The flowchart of the proposed methodology is shown in Fig. 1.

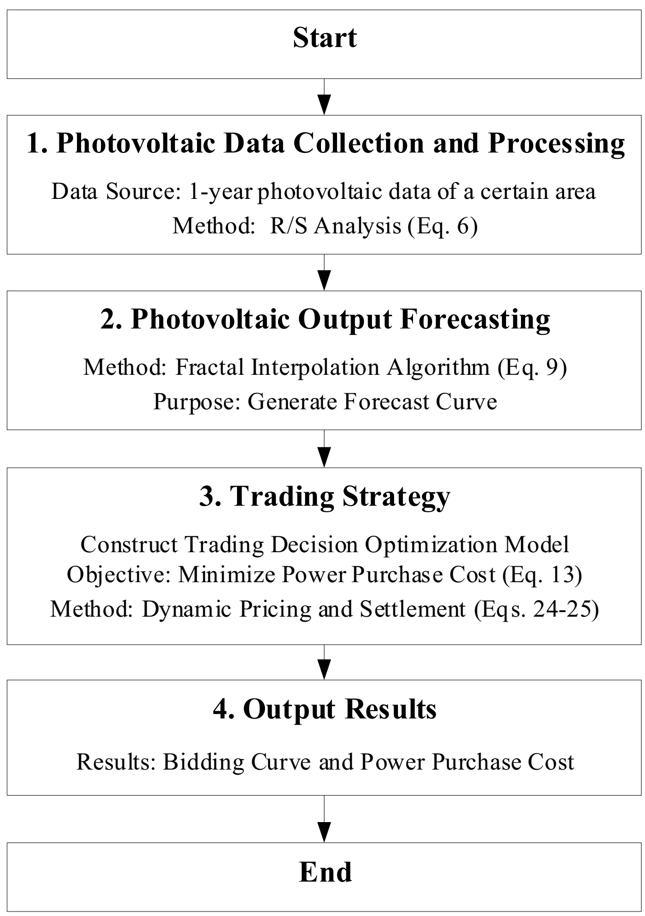

Figure 1: The flowchart of the proposed methodology

3 Results

3.1 Analysis of Fractal Characteristics of PV Output under Different Weather Conditions

By taking the data of sunny, cloudy and rainy days in a certain location as an example, the fractal characteristics of PV output are analyzed. In Fig. 2, the PV output under the three weather conditions shows obvious nonlinear characteristics. During the analysis process, a set of data is recorded every 15 min, and each set of data has a length of 96. Using R/S analysis, the PV fractal curve is obtained as shown in Fig. 3. It can be seen that the fractal curves of PV output under each weather condition are also constantly changing, but the overall trend is close to linearity. The fractal results of the three weather conditions are shown in Table 1.

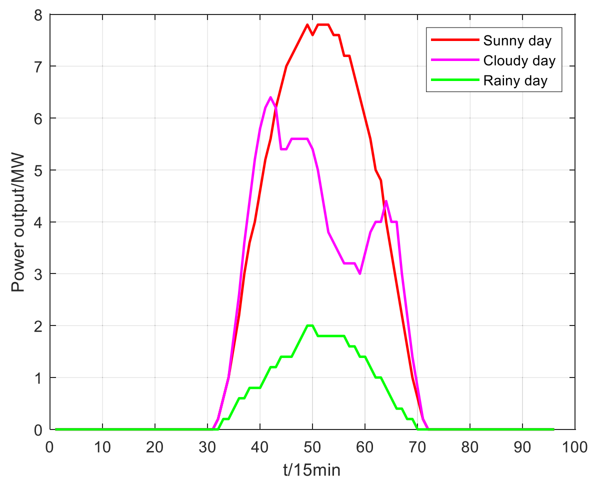

Figure 2: PV output curves under different weather conditions

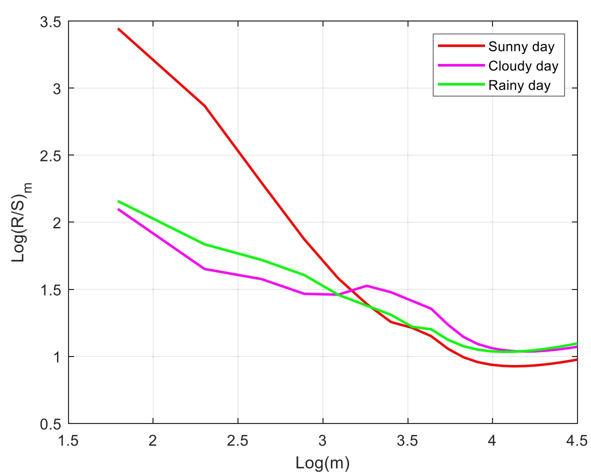

Figure 3: The fractal curve of PV output under different weather conditions

Table 1: The fractal dimension results under different weather conditions

Weather	Sunny day	Cloudy day	Rainy day
Dimensional value	1.5611	1.6129	1.6139

From the results in Fig. 3 and Table 1, it can be seen that the fractal dimensions of the PV output vary under different weather conditions. The fractal dimension is the highest on rainy and cloudy days, at 1.6139, followed by overcast days, at 1.6129, and the lowest on sunny days, at 1.5611. This indicates that under rainy and cloudy weather conditions, the volatility and complexity of the PV output are relatively higher, and the anti-persistence characteristics are more obvious. Combined with the analysis of the Hurst index, it can be inferred that under different weather conditions, the PV output shows a certain degree of mean reversion characteristic, that is, there are local fluctuations that are opposite to the overall trend.

The self-similarity of the PV output for the two consecutive weeks is analyzed below. The continuous two-week PV output data of this location are shown in Fig. 4. As can be seen from Fig. 4, the fluctuations of the PV output over the two consecutive weeks are large, and they include different weather types. Using R/S analysis, the fractal dimension curve is obtained as shown in Fig. 5, and the fractal dimension results are shown in Table 2.

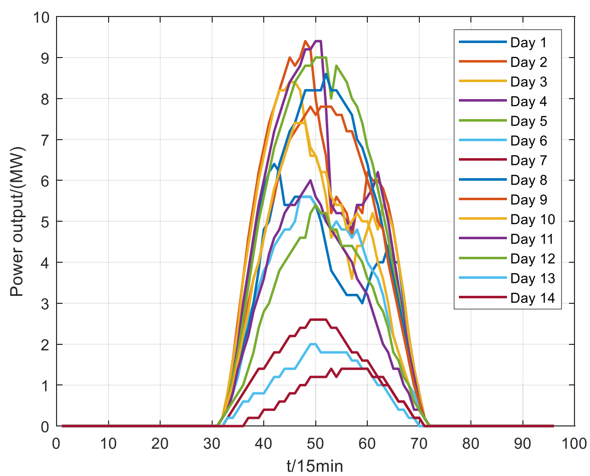

Figure 4: The continuous two-week PV output data

From Fig. 5 and Table 2, it can be seen that the fractal dimension values of the PV output under different weather conditions vary to some extent, but overall they exhibit relatively stable fractal characteristics. Over a two-week period, although the weather conditions were variable, including sunny, cloudy, and overcast days, the fractal dimension results of the PV output showed certain regularity. From the data, the fractal dimension result on day 9 was 1.5403, which was the day with a relatively higher fractal dimension value during these two weeks, possibly indicating that the weather conditions on that day made the fluctuation of PV output more complex, and the self-similarity feature was relatively less obvious. While the fractal dimension results on day 2 and day 8 were relatively lower, being 1.4174 and 1.4081, respectively, which indicated that the self-similarity of the PV output on these two days might be stronger, and the fluctuation of output was relatively more regular. Regardless of the type of weather, the fractal dimension values of the PV output mostly fluctuated between 1.4 and 1.55, indicating that although the weather conditions were variable, the self-similarity feature of the PV output remained significant.

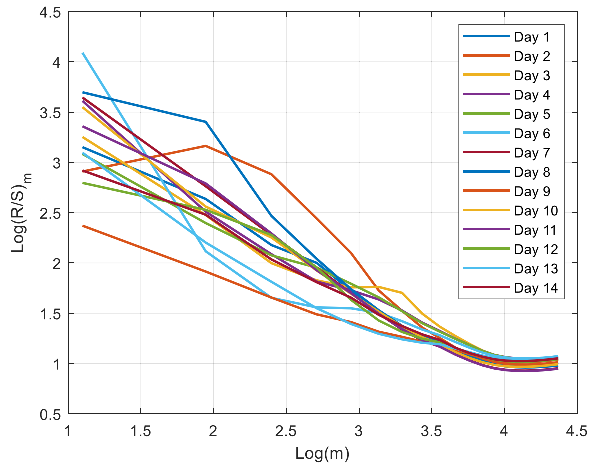

Figure 5: The continuous two-week fractal curve of PV output

Table 2: The continuous two-week fractal dimension results of PV output

Time period	Fractal dimension	Time period	Fractal dimension
Day 1	1.4584	Day 8	1.4081
Day 2	1.4174	Day 9	1.5403
Day 3	1.4394	Day 10	1.4449
Day 4	1.4272	Day 11	1.4531
Day 5	1.4509	Day 12	1.4753
Day 6	1.4385	Day 13	1.4928
Day 7	1.4403	Day 14	1.475

The Hurst index, as a key indicator for quantifying the long-term memory of a time series, its value directly reflects the fluctuation characteristics of the photovoltaic output sequence. When the H value is close to 0.5, the sequence approaches random walk, and the prediction uncertainty increases; when the H value deviates from 0.5, the sequence exhibits persistence or anti-persistence. Particularly, sequences with significant persistence ($H > 0.5$) are more predictable due to their trend continuation characteristics, while sequences with strong anti-persistence ($H < 0.5$) will increase the difficulty of prediction due to their frequent mean reversion behavior. Therefore, there is an inherent theoretical correlation between the Hurst index and the prediction accuracy, and the sequence characteristics corresponding to different H values will directly affect the error level of subsequent fractal interpolation prediction.

3.2 Analysis of Typical Day PV Output Prediction

Based on the above analysis, the PV output sequence has the characteristic of daily similarity. Next, using the fractal interpolation algorithm, the PV output on day 5 of the typical day is predicted based on the 4-day PV output data of the typical day.

The 4-day PV output data of the typical day is shown in Fig. 6. Since the typical day PV output curve is selected, the PV output data of these 4 days exhibit certain regularity and similarity. The fractal interpolation algorithm was used to predict the PV output on day 5, and the comparison results are shown in Fig. 7. As can be seen from Fig. 7, the predicted curve demonstrates strong agreement with the actual output curve. During the morning and evening periods when PV output remains relatively low, the deviation between predicted and actual values is minimal. Although certain discrepancies exist around noon when PV output peaks, the overall trends remain consistent. This indicates that the fractal interpolation algorithm effectively captures the daily similarity characteristics of PV output, demonstrating considerable accuracy and reliability in predicting typical daily PV generation patterns.

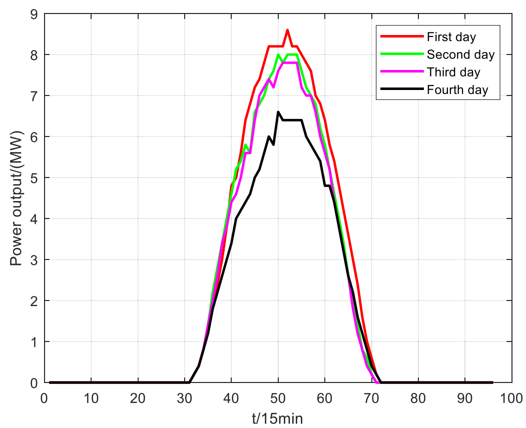

Figure 6: The 4-day PV output data for typical days

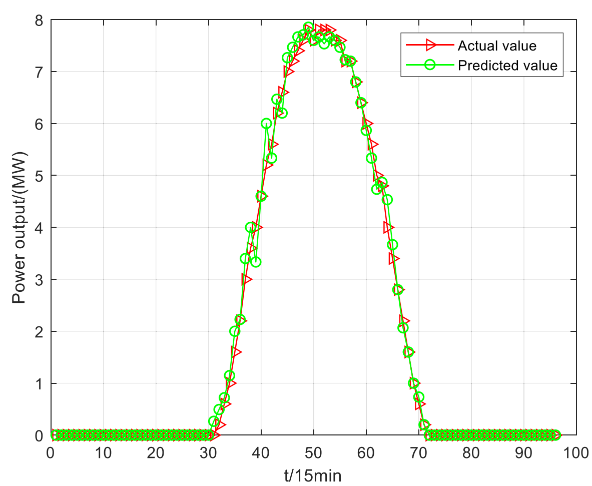

Figure 7: Comparison between predicted and actual PV output on typical day 5

To verify the superiority of the fractal interpolation method in predicting photovoltaic output, this section further compares it with the ARIMA model and the LSTM neural network, and the comparison results are shown in Fig. 8. As can be seen from Fig. 8, under the same dataset and prediction conditions, the matching degree between the prediction curve of the fractal interpolation method and the actual output curve is significantly higher than that of the ARIMA model and the LSTM neural network. Especially during periods with large fluctuations in solar power output, the fractal interpolation method can more accurately capture the trend of output changes, while the ARIMA model and the LSTM neural network have certain lag and deviations, indicating that the fractal interpolation method has stronger adaptability and prediction accuracy when dealing with solar power output data with fractal characteristics.

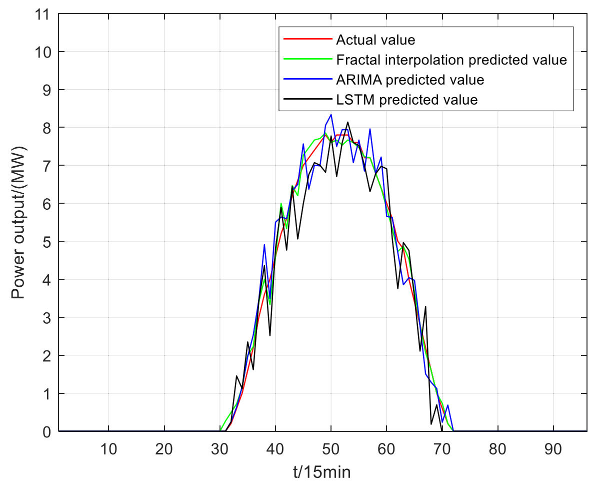

Figure 8: Comparison of predicted and actual values of photovoltaic power output by different methods

3.3 Analysis of PV Output Optimization

Taking a certain industrial park as an example for analysis, it is known that the installed capacity of PV power in this park is 20 MW. Under the market-based trading mechanism, the park has engaged an electricity retail company as its unified agent. This company is responsible for coordinating the electricity demand of park users and the output of distributed PV generation, while also representing the park in purchasing and selling electricity in the spot market. Based on the typical day operational data of the park shown in Fig. 9, its load profile exhibits distinct peak-valley differences. The maximum daily load demand reaches 72 MW, while the average daily load remains at approximately 44 MW. The predicted electricity price fluctuates within a range of 76–264 RMB/(MW·h), with a daily average price of 151 RMB/(MW·h). During the evening peak consumption period from 18:00 to 23:00, prices remain consistently high, averaging 243 RMB/(MW·h). In order to enhance the economic benefits and dispatchability of PV power generation, the PV operator has deployed an energy storage system, with relevant parameters provided in Table 3.

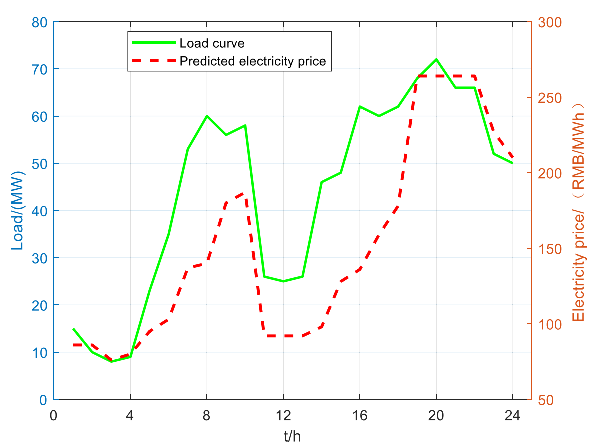

Figure 9: The typical day load curve and predicted electricity price

Table 3: Relevant parameters of energy storage system

Name	Parameter
Capacity (MW·h)	100
Charging power (MW)	10
Discharging power (MW)	10
Charge-discharge efficiency (%)	0.9
$\left[S_{\mathrm{SOC}}^{\min}, S_{\mathrm{SOC}}^{\max}\right]$	[0.1, 0.9]
Initial state of charge	0.5

In the market-oriented trading environment, based on electricity price forecasting results and following the price decision mechanism proposed in this paper, the electricity retail company and distributed PV power producers can determine an optimized decision price range of 151–243 RMB/(MW·h) for their transactions. To systematically study the impact of price decisions on trading behaviors, this paper selects three price points for comparative analysis: 160 RMB/(MW·h) (Scenario 1), 200 RMB/(MW·h) (Scenario 2), and 240 RMB/(MW·h) (Scenario 3). Under different decision prices, the electricity retail company will adjust its spot market procurement strategy accordingly, while PV power producers will optimize their power generation schedules and reasonably dispatch the charging and discharging strategies of their supporting energy storage systems.

Through systematic analysis and strategy optimization, a comparison of PV output before and after optimization of three scenarios is obtained, as shown in Fig. 10. It can be seen that when the decision price falls within the range between the daily average price and the evening peak average price, the optimization results across the three scenarios show high similarity. The PV utilization rates under different decision prices all exceed 60%, indicating that fluctuations in price parameters within a reasonable range have a certain impact on the overall renewable energy utilization rate of the system.

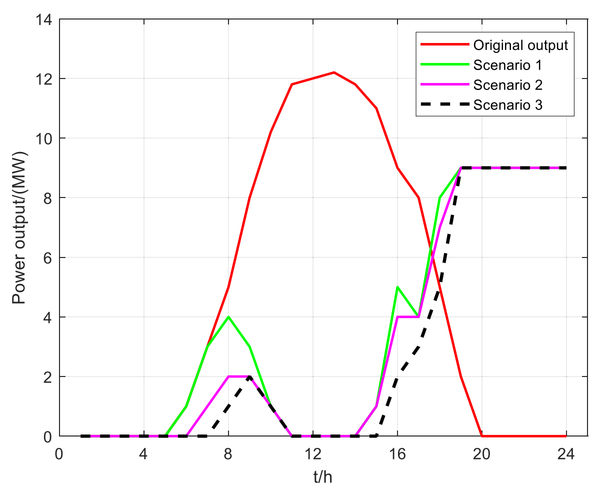

Figure 10: Comparison of PV output before and after optimization of three scenarios

By taking the decision-making price of Scenario 2 as an example, through the optimized calculation of the transaction decision-making model, the declaration curve of electricity retail company in the spot market is shown in Fig. 11. It can be seen that during the evening peak electricity price period, the declared electricity quantity drops significantly. This change trend highly coincides with the discharge behavior of the energy storage system and the optimized result of the PV power output, which indicates that through the spatial-temporal energy transfer capability of the energy storage system, the PV power during the low-price period at noon is transferred to the high-price period in the evening for use. Thus, while meeting the user demand, the minimization of the power purchase cost is achieved, which further proves that the transaction decision-making model proposed in this paper can effectively coordinate the PV power output and market demand, and improve the efficiency of power resource allocation.

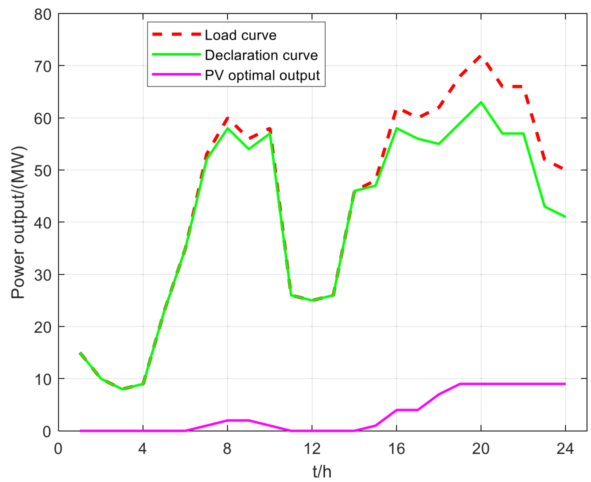

Figure 11: Declaration curve of electricity retail company in spot market under Scenario 2

The Hurst index of the photovoltaic output sequence has an important impact on the optimization effect of the market strategy by influencing the prediction accuracy. The analysis shows that when the H value significantly deviates from 0.5, the trading strategy based on high-precision prediction can more accurately coordinate the consumption of photovoltaic power and the purchase of electricity in the spot market, achieving better economic performance.

3.4 Analysis of Electricity Procurement Cost

In order to systematically study the economic impact of electricity price prediction deviations on market entities, this paper sets up two actual electricity price scenarios as shown in Fig. 12.

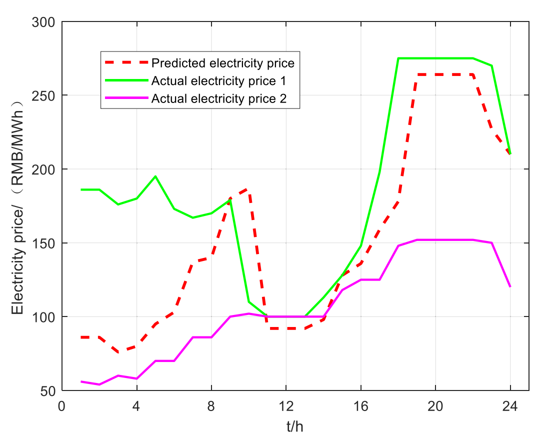

Figure 12: Predicted electricity price and two actual electricity price curves

Actual electricity price scenario 1 represents the conservative estimation situation where the predicted electricity price is lower than the actual electricity price, and actual electricity price scenario 2 corresponds to the optimistic estimation situation where the predicted electricity price is higher than the actual electricity price. These two scenarios respectively reflect the phenomena of overestimation and underestimation of electricity prices that may occur in the electricity market. The average daily electricity price of actual electricity price scenario 1 is 186 RMB/(MW·h), and the average electricity price during the evening peak is 274 RMB/(MW·h). The average daily electricity price of actual electricity price scenario 2 is 105 RMB/(MW·h), and the average electricity price during the evening peak is 151 RMB/(MW·h). By using the proposed settlement price mechanism, differentiated contract settlement prices are established for PV power producers and electricity retailers as specified in Table 2.

Based on the settlement prices under the two actual electricity price scenarios shown in Table 4, the optimized procurement costs for the three scenarios are presented in Figs. 13 and 14, respectively. From Fig. 13, it can be observed that under settlement scenario 1 with actual electricity prices, as the electricity load increases in market transactions, the procurement costs of the retail company show an upward trend. However, through the implementation of the optimization strategy proposed in this paper, the rate of cost increase is effectively controlled, demonstrating a significant reduction compared to the unoptimized scenario.

Table 4: Contract settlement prices of the two actual electricity prices

Scenario	Settlement prices				
Actual electricity price 1	190	210	230	250	270
Actual electricity price 2	110	120	130	140	150

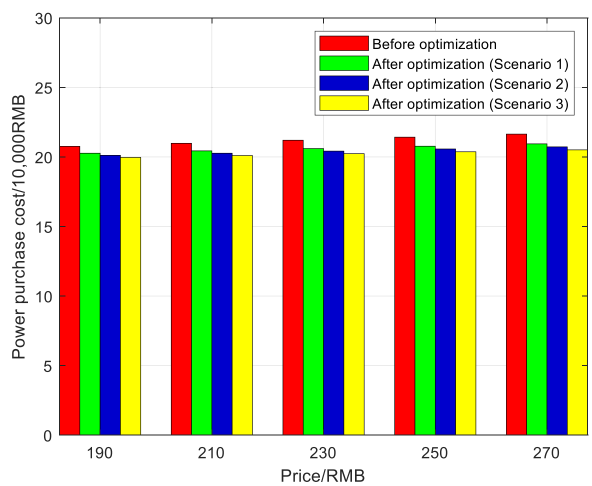

Figure 13: Power purchase cost in the settlement scenario of actual electricity price 1

As shown in Fig. 14, under settlement scenario 2 with actual electricity prices, procurement costs also rise with increasing electricity load. Nevertheless, due to the generally lower actual electricity prices in this scenario, the absolute cost values remain relatively low. Moreover, the optimization strategy continues to function effectively, further reducing procurement expenditures and enabling the retail company to achieve favorable economic performance even in this context.

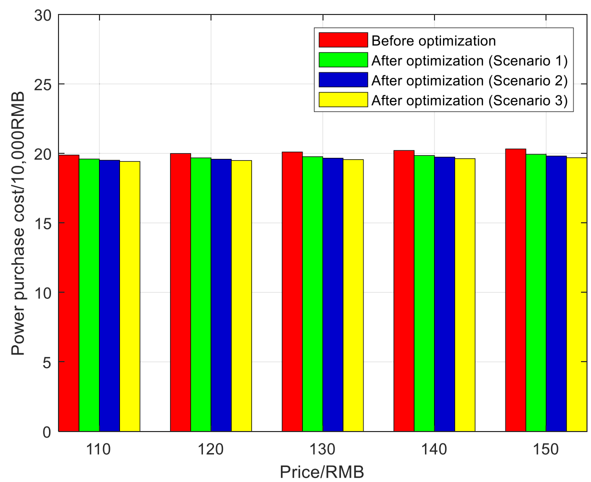

Figure 14: Power purchase cost in the settlement scenario of actual electricity price 2

4 Conclusions

This paper focuses on the issue of output fluctuation and power purchase decision optimization brought about by the integration of distributed PV power, and proposes a PV output prediction and trading strategy based on fractal theory. Through theoretical analysis and case verification, the following conclusions are drawn: The PV output time series exhibits significant fractal characteristics and self-similarity under different weather conditions, and the complexity of its fluctuations can be quantitatively characterized by the fractal dimension. Based on this feature, the fractal interpolation prediction model can effectively capture the intrinsic change patterns of PV output and achieve high-precision fitting of the typical day output curve. Compared with traditional ARIMA and LSTM methods, the fractal interpolation method can more accurately describe the nonlinear fluctuation characteristics of photovoltaic output, with smaller prediction errors, and requires less data input and has a strong model interpretability. In addition, the power purchase company cost model, trading decision model, and dynamic pricing and settlement mechanism constructed by integrating the fractal prediction results can collaboratively optimize the PV consumption and power purchase costs. Combined with the charging and discharging scheduling of the energy storage system, it can mitigate the impact of spot price fluctuations and effectively improve the PV consumption rate and reduce the power purchase costs of the power purchase company.

Further research can explore how to apply fractal theory to the output prediction and trading strategy formulation of other renewable energy sources, construct more comprehensive and flexible decision models, and better serve the sustainable development of distributed PV and the stable operation of the power market.

Acknowledgement: Not applicable.

Funding Statement: This research was supported by the Science and Technology Project Funding of State Grid Corporation of China: Key Technology Research and Application of Hierarchical Control and Consumption for Low-Voltage Distributed Photovoltaics (5400-202313567A-3-2-ZN).

Author Contributions: The authors confirm their contribution to the paper as follows: Conceptualization, methodology, project administration, writing—original draft, and funding acquisition: Yifeng Wang; conceptualization, investigation: Wei Cui; methodology, software: Zhihui Wang; formal analysis, validation: Yanning Xue; writing—original draft, writing—review & editing: Bing Wang. All authors reviewed the results and approved the final version of the manuscript.

Availability of Data and Materials: The authors confirm that the data supporting the findings of this study are available within the article. And the additional data that support the findings of this study are available on request from the corresponding author, upon reasonable request.

Ethics Approval: Not applicable.

Conflicts of Interest: The authors declare no conflicts of interest to report regarding the present study.

References

1. Kang K, Jia H, Hui H, Liu D. Two-stage optimization configuration of shared energy storage for multi-distributed photovoltaic clusters in rural distribution networks considering self-consumption and self-sufficiency. Appl Energy. 2025;394:126174. doi:10.1016/j.apenergy.2025.126174.
2. Wang S, Hou Y, Guan X, Liu S, Huo Z. Resiliency-informed optimal scheduling of smart distribution network with urban distributed photovoltaic: a stochastic P-robust optimization. Energy. 2024;313:133449. doi:10.1016/j.energy.2024.133449.
3. Sun D, Cao X, Liang Z, Xia J, Wang Y. Distributed photovoltaic power prediction technology based on spatio-temporal graph neural networks. Energy Eng. 2025;122(8):3329–46. doi:10.32604/ee.2025.066341.
4. Li W, Dong F, Ji Z, Wang P. Internal and external coordinated distributionally robust bidding strategy of virtual power plant operator participating in day-ahead electricity spot and peaking ancillary services markets. Appl Energy. 2025;386:125514. doi:10.1016/j.apenergy.2025.125514.
5. Goyal A, Bhattacharya K. Design of multi-settlement electricity markets considering demand response and battery energy storage systems participation. IEEE Trans Energy Mark Policy Regul. 2024;2(2):226–39. doi:10.1109/TEMPR.2024.3350510.
6. Dvorkin V. Regression equilibrium in electricity markets. IEEE Trans Energy Mark Policy Regul. 2025;3(1):121–32. doi:10.1109/TEMPR.2025.3530266.
7. Simoglou CK, Biskas PN, Tsoumalis GI, Papalexopoulos AD. Exploring and quantifying the impact of ex-ante market power mitigation in the integrated European day-ahead electricity market. IEEE Trans Energy Mark Policy Regul. 2025;3(1):83–97. doi:10.1109/TEMPR.2024.3500068.
8. Wang C, Wu Z, Wei L, Yang L, Zhang Y, Yuan B, et al. Evaluating the externality value of distributed photovoltaics: industry-specific investment decisions under diverse pricing schemes. Renew Energy. 2025;247(10):122986. doi:10.1016/j.renene.2025.122986.
9. Zhang K, Cui Y, Wei Y, Wang W, Yue Y, Zhang Y. Research on distributed photovoltaic efficient digestion method based on optical storage direct flexible mode. Energy Rep. 2025;13(24):4926–35. doi:10.1016/j.egyr.2025.04.018.
10. Wang Y, Huang W, Chen H, Yu Z, Hu L, Huang Y. Optimal scheduling strategy for virtual power plants with aggregated user-side distributed energy storage and photovoltaics based on CVaR-distributionally robust optimization. J Energy Storage. 2024;86(1):110770. doi:10.1016/j.est.2024.110770.
11. Chen D, Mei M, Jiang J, Wang C. A segmented fractal model associated with the spatial distribution characteristics of urban rail transit network. Chaos Solitons Fractals. 2025;194(5):116113. doi:10.1016/j.chaos.2025.116113.
12. Budanov P, Kyrysov I, Brovko K, Rudenko D, Vasiuchenko P, Nosyk A. Development of a solar element model using the method of fractal geometry theory. East Eur J Enterp Technol. 2021;3(8(111)):75–89. doi:10.15587/1729-4061.2021.235882.
13. Zhu J. Drag and uncertainty of power-law fluid flows in fractal multiparticle systems. Powder Technol. 2023;428(2):118838. doi:10.1016/j.powtec.2023.118838.
14. Fu Y, Xu L, Li Y, Yang EJ, Guo Y, Cai G, et al. Enhancing inter-domain connectivity by reducing fractal dimensions: the key to passivating deep traps in organic photovoltaics. Energy Environ Sci. 2024;17(22):8893–903. doi:10.1039/d4ee02961e.
15. He L, Zhang J. Energy trading in local electricity markets with behind-the-meter solar and energy storage. IEEE Trans Energy Mark Policy Regul. 2023;1(2):107–17. doi:10.1109/TEMPR.2023.3250948.

16. Jiang ZQ, Xie WJ, Zhou WX, Sornette D. Multifractal analysis of financial markets: a review. Rep Prog Phys. 2019;82(12):125901. doi:10.1088/1361-6633/ab42fb.
17. Zhang QM, Chen LJ, Li XZ, Mei SW. Optimization decision of purchasing and selling power between industrial park operators and distributed optical storage users based on Stackelberg game. Acta Energiae Solaris Sin. 2024;45(1):450–6. (In Chinese). doi:10.19912/j.0254-0096.tynxb.2022-1527.
18. Wei Z, Liu J, Tang Z, Liu Y, Jawad S, Liu J, et al. A comprehensive competitiveness decision method for electricity retailers considering the integration of device operation, investment planning, and marketing strategy. IEEE Syst J. 2024;18(1):244–55. doi:10.1109/JSYST.2023.3328004.
19. Guo Q, Wang X, Tu C, Che L, Xiao F, Hou Y. A multitimescale energy management strategy for advanced cophase traction power supply system with PV and ES. IEEE Trans Transp Electrif. 2025;11(1):859–69. doi:10.1109/TTE.2024.3396878.
20. Li J, Guo Q, Wang X, Tu C, Che L, Xiao F, et al. A real-time hierarchical energy management strategy for FTPSS to improve the PV/RBE utilization and power supply quality. IEEE Trans Intell Transp Syst. 2025;26(1):1203–14. doi:10.1109/TITS.2024.3489673.
21. Feng R, Wang K, Xu X, Yu ZT, Lin Q. Triple-layer optimization of distributed photovoltaic energy storage capacity for manufacturing enterprises considering carbon emissions and load management. Appl Energy. 2024;364(32):123164. doi:10.1016/j.apenergy.2024.123164.
22. Liu J, Luo X, Liu X, Gao Y, Zhou T, Zhai X, et al. Study on multi-agent evolutionary games promoting "distributed photovoltaics and electric heating" in rural areas: a case study in Xi'an, China, a pilot city for clean heating. J Clean Prod. 2025;486(2):144458. doi:10.1016/j.jclepro.2024.144458.
23. Jia Q, Li Y, Yan Z, Chen S. Reactive power market design for distribution networks with high photovoltaic penetration. IEEE Trans Smart Grid. 2023;14(2):1642–51. doi:10.1109/TSG.2022.3186338.
24. Zhao SQ, Song JL, Wang AE, Liao YM, Li ZW. Design of electricity spot market trading mechanism considering high proportion of new energy consumption and peak load adjustment compensation of thermal power units. Acta Energiae Solaris Sin. 2024;45(8):164–73. (In Chinese). doi:10.19912/j.0254-0096.tynxb.2023-0585.
25. Li Z, Ma T. Distributed photovoltaics with peer-to-peer electricity trading. Energy Built Environ. 2022;3(4):424–32. doi:10.1016/j.enbenv.2021.04.004.
26. Yang S, Wang X, Yang Y, Li J. Bi-level planning model of distributed PV-energy storage system connected to distribution network under the coordinated operation of electricity-carbon market. Sustain Cities Soc. 2023;89(102117):104347. doi:10.1016/j.scs.2022.104347.
27. Hu H, Tan D, Thaichon P, Wang B, Zhu Z. Grid-based market sales forecasting for retail businesses using automated machine learning and geospatial intelligence. Expert Syst Appl. 2025;284(5–6):127869. doi:10.1016/j.eswa.2025.127869.
28. Liao P, Liu H, Wang Y, Liao N. Optimization of electricity purchase and sales strategies of electricity retailers under the condition of limited clean energy consumption. Energy Eng. 2023;120(3):701–14. doi:10.32604/ee.2022.024301.
29. Mansouri SA, Maroufi S, Ahmarinejad A. A tri-layer stochastic framework to manage electricity market within a smart community in the presence of energy storage systems. J Energy Storage. 2023;71:108130. doi:10.1016/j.est.2023.108130.
30. Wang B, Xu X, Li G, Fan H, Qiao N, Chen H, et al. A study of electricity sales offer strategies applicable to the participation of multi-energy generators in short- and medium-term markets. Sustain Energy Grids Netw. 2024;40(2):101553. doi:10.1016/j.segan.2024.101553.